Journal of the American College of Cardiology
© 2013 by the American College of Cardiology Foundation
Published by Elsevier Inc.

Vol. 62, No. 19, 2013
ISSN 0735-1097/$36.00
http://dx.doi.org/10.1016/j.jacc.2013.05.071

Cardiac Imaging

In Vivo Diagnosis of Plaque Erosion and Calcified Nodule in Patients With Acute Coronary Syndrome by Intravascular Optical Coherence Tomography

Haibo Jia, MD, PhD,*† Farhad Abtahian, MD, PhD,† Aaron D. Aguirre, MD, PhD,‡ Stephen Lee, MD,§ Stanley Chia, MD,‖ Harry Lowe, MBChB, PhD,¶ Koji Kato, MD, PhD,† Taishi Yonetsu, MD,† Rocco Vergallo, MD,† Sining Hu, MD,*† Jinwei Tian, MD, PhD,*† Hang Lee, PhD,# Seung-Jung Park, MD, PhD,** Yang-Soo Jang, MD, PhD,†† Owen C. Raffel, MD,‡‡ Kyoichi Mizuno, MD, PhD,§§ Shiro Uemura, MD, PhD,‖‖ Tomonori Itoh, MD,¶¶ Tsunekazu Kakuta, MD,## So-Yeon Choi, MD, PhD,*** Harold L. Dauerman, MD,††† Abhiram Prasad, MD,‡‡‡ Catalin Toma, MD,§§§ Iris McNulty, RN,† Shaosong Zhang, MD, PhD,‖‖‖ Bo Yu, MD, PhD,* Valentine Fuster, MD, PhD,¶¶¶ Jagat Narula, MD, PhD,¶¶¶ Renu Virmani, MD,### Ik-Kyung Jang, MD, PhD†

Harbin and Hong Kong, China; Boston, Massachusetts; Singapore; Sydney and Brisbane, Australia; Seoul and Suwon, Republic of Korea; Tokyo, Nara, Morioka, and Tsuchiura, Japan; Burlington, Vermont; Rochester, Minnesota; Gaithersburg, Maryland; Pittsburgh, Pennsylvania; and New York, New York

Objectives The aim of this study was to characterize the morphological features of plaque erosion and calcified nodule in patients with acute coronary syndrome (ACS) by optical coherence tomography (OCT).

Background Plaque erosion and calcified nodule have not been systematically investigated in vivo.

Methods A total of 126 patients with ACS who had undergone pre-intervention OCT imaging were included. The culprit lesions were classified as plaque rupture (PR), erosion (OCT-erosion), calcified nodule (OCT-CN), or with a new set of diagnostic criteria for OCT.

Results The incidences of PR, OCT-erosion, and OCT-CN were 43.7%, 31.0%, and 7.9%, respectively. Patients with OCT-erosion were the youngest, compared with those with PR and OCT-CN (53.8 ± 13.1 years vs. 60.6 ± 11.5 years, 65.1 ± 5.0 years, $p = 0.005$). Compared with patients with PR, presentation with non–ST-segment elevation ACS was more common in patients with OCT-erosion (61.5% vs. 29.1%, $p = 0.008$) and OCT-CN (100% vs. 29.1%, $p < 0.001$). The OCT-erosion had a lower frequency of lipid plaque (43.6% *vs.* 100%, $p < 0.001$), thicker fibrous cap (169.3 ± 99.1 μm vs. 60.4 ± 16.6 μm, $p < 0.001$), and smaller lipid arc (202.8 ± 73.6° vs. 275.8 ± 60.4°, $p < 0.001$) than PR. The diameter stenosis was least severe in OCT-erosion, followed by OCT-CN and PR (55.4 ± 14.7% vs. 66.1 ± 13.5% vs. 68.8 ± 12.9%, $p < 0.001$).

Conclusions Optical coherence tomography is a promising modality for identifying OCT-erosion and OCT-CN in vivo. The OCT-erosion is a frequent finding in patients with ACS, especially in those with non–ST-segment elevation ACS and younger patients. The OCT-CN is the least common etiology for ACS and is more common in older patients. (The Massachusetts General Hospital Optical Coherence Tomography Registry; NCT01110538) (J Am Coll Cardiol 2013;62:1748–58) © 2013 by the American College of Cardiology Foundation

From the *Department of Cardiology, The 2nd Affiliated Hospital of Harbin Medical University, The Key Laboratory of Myocardial Ischemia, Chinese Ministry of Education, Harbin, China; †Cardiology Division, Massachusetts General Hospital, Harvard Medical School, Boston, Massachusetts; ‡Cardiovascular Division, Brigham and Women's Hospital, Harvard Medical School, Boston, Massachusetts; §Department of Medicine, Queen Mary Hospital, Hong Kong University, Hong Kong, China; ‖National Heart Centre Singapore, Singapore; ¶Concord Repatriation General Hospital, Sydney, Australia; #Biostatistics, Massachusetts General Hospital, Harvard Medical School, Boston, Massachusetts; **Asan Medical Center, Seoul, Republic of Korea; ††Severance Cardiovascular Hospital, Yonsei University, Seoul, Republic of Korea; ‡‡Prince Charles Hospital, Brisbane, Australia; §§Department of Cardiovascular Medicine, Nippon Medical School, Tokyo, Japan; ‖‖Nara Medical

Coronary thrombosis is the most frequent final event leading to an acute coronary syndrome (ACS). The 3 most common underlying mechanisms contributing to ACS are believed to be plaque rupture (PR), plaque erosion, and calcified nodule (1,2). Plaque rupture is the most frequent finding in autopsy studies of patients with sudden cardiac death (SCD) (1,3,4). However, a significant portion of thrombotic lesions found on autopsy are not associated with an underlying PR. In a series of 20 case subjects with SCD, van der Wal et al. (5) found PR in only 60% of lesions; the remaining 40% showed only plaque erosion without rupture. Virmani et al. (1) studied over 200 cases of SCD. Only one-third of lesions could be described as PR, and 35% of lesions with thrombi failed to show rupture. A more recent autopsy study reported that approximately two-thirds (69%) of SCD cases showed organizing or healing thrombi, of which 88% were caused by erosion (6). The least common pathological finding associated with thrombosis is calcified nodules. Calcified nodules are pathologically defined as the presence of fracture of a calcified plate, interspersed fibrin, and a disrupted fibrous cap with an overlying thrombus (1,3). The frequency of erosion and calcified nodule might be underestimated in patients with ACS due to the lack of diagnostic modalities that readily identify them.

See page 1759

Optical coherence tomography (OCT) is an emerging intravascular imaging modality with a resolution of 10 to 20 μm. It can visualize the microstructure of atherosclerotic plaque (such as fibrous cap, thrombus, and calcification), and the OCT characteristics were validated by histology (7,8). Pathologically, plaque erosion is defined as a loss of endothelial lining with lacerations of the superficial intimal layers in the absence of "trans-cap" ruptures (1). However, OCT does not provide adequate resolution to identify the endothelial lining. Therefore, the pathological definition of erosion cannot simply be adapted for the OCT definition. In addition, calcified nodules have never been systematically studied by OCT.

The aim of our study was to evaluate the morphological characteristics of OCT-determined plaque erosion (OCT-erosion) and calcified nodules (OCT-CN) in patients with ACS (including ST-segment elevation myocardial infarction [STEMI] and non–ST-segment elevation acute coronary syndrome [NSTE-ACS]).

Abbreviations and Acronyms

ACS = acute coronary syndrome(s)
ECG = electrocardiogram
MI = myocardial infarction
NSTE-ACS = non–ST-segment elevation acute coronary syndrome
NSTEMI = non–ST-segment elevation myocardial infarction
OCT = optical coherence tomography
STEMI = ST-segment elevation myocardial infarction
SCD = sudden cardiac death

Methods

Study population. The Massachusetts General Hospital OCT Registry is a multicenter registry of patients undergoing OCT imaging of the coronary arteries and includes 20 sites across 6 countries. We selected patients with ACS who have undergone pre-intervention OCT imaging of culprit lesions from the registry. Of 206 ACS patients, 126 were included for analysis. The remaining 80 cases were excluded for the following reasons: pre-dilation (n = 38), previous stent implantation in the culprit vessel (n = 27), left main disease (n = 2), massive thrombus (n = 6), and poor image quality (n = 7).

The patients with ACS consisted of STEMI and NSTE-ACS. ST-segment elevation myocardial infarction (MI) was defined as continuous chest pain that lasted >30 min, arrival at the hospital within 12 h from the onset of symptoms, ST-segment elevation >0.1 mV in >2 contiguous leads or new left bundle-branch block on the 12-lead electrocardiogram (ECG), and elevated cardiac markers (creatine kinase-myocardial band or troponin T/I). The NSTE-ACS included non–ST-segment elevation myocardial infarction (NSTEMI) and unstable angina pectoris. NSTEMI was defined as ischemic symptoms in the absence of ST-segment elevation on the ECG with elevated cardiac markers. Unstable angina pectoris was defined as having newly developed/accelerating chest symptoms on exertion or rest angina within 2 weeks. The culprit lesion was identified on the basis of coronary angiogram, stress test, ECG, left ventriculogram, or echocardiogram. The protocol for the registry was approved by the institutional review board of each site, and all patients provided informed consent.

University, Nara, Japan; ¶¶Division of Cardiology, Memorial Heart Center, Iwate Medical School, Morioka, Japan; ##Tsuchiura Kyodo General Hospital, Tsuchiura, Japan; ***Ajou University Hospital, Suwon, Republic of Korea; †††Division of Cardiology, University of Vermont College of Medicine/Fletcher Allen Healthcare, Burlington, Vermont; ‡‡‡Division of Cardiovascular Diseases, Department of Internal Medicine, Mayo Clinic, Rochester, Minnesota; §§§University of Pittsburgh Medical Center, Pittsburgh, Pennsylvania; ||||LightLab Imaging, Inc./St. Jude Medical, Westford, Massachusetts; ¶¶¶Mount Sinai Hospital, New York, New York; and the ###Cardiovascular Pathology Institute, Gaithersburg, Maryland. This study was supported by research grants from St. Jude Medical, the Cardiology Division of Massachusetts General Hospital. Dr. Jia has received a grant from the National Natural Science Foundation of China (grant contract number: 81200076) and Open Foundation of Key Laboratory of Myocardial Ischemia (Harbin Medical University), Chinese Ministry of Education (KF201205). Dr. Aguirre is funded by National Institute of Health T32HL094301. Dr. Vergallo has received a grant from the Enrico ed Enrica Sovena Foundation, Italy. Dr. Dauerman has served as consultant to Medtronic and The Medicines Company; and has received research grants from Abbott Vascular and Medtronic. Dr. Zhang is an employee of St. Jude Medical. Dr. Yu has received a grant from the National Natural Science Foundation of China (grant contract number: 30871064/C140401). Dr. Virmani has received research support from Abbott Vascular, BioSensors International, Biotronik, Boston Scientific, Medtronic, MicroPort Medical, OrbusNeich Medical, SINO Medical Technology, and Terumo Corporation; honoraria from Abbott Vascular, Boston Scientific, Terumo Corporation, and Lutonix; served as consultant to Abbott Vascular, 480 Biomedical, and WL Gore; and served on the speakers' bureau for Merck. Dr. Jang has received research grants and consulting fees from LightLab Imaging/St. Jude Medical. All other authors have reported that they have no relationships relevant to the contents of this paper to disclose. Stephen Nicholls, MBBS, PhD, served as Guest Editor for this article.

Manuscript received February 17, 2013; revised manuscript received May 2, 2013, accepted May 22, 2013.

OCT image acquisition. The OCT imaging of culprit lesions was acquired with either the commercially available time-domain (M2/M3 Cardiology Imaging System, Lightlab Imaging/St. Jude Medical, Westford, Massachusetts) or frequency-domain OCT C7XR system and the Dragon Fly catheter (Lightlab Imaging/St. Jude Medical). Patients requiring pre-dilation and aspiration thrombectomy before OCT imaging were excluded. In the M2/M3 system, an occlusion balloon (Helios, LightLab Imaging) was inflated proximal to the lesion at 0.4 to 0.6 atm during image acquisition. The optical probe was automatically pulled back from distal to proximal at a rate of 1.0 to 3.0 mm/s, and saline was continuously infused from the tip of the occlusion balloon. In the C7XR system, a 2.7-F OCT imaging catheter was carefully advanced distal to the culprit lesion. The automated pullback was performed at 20 mm/s, while blood was displaced by a short injection of contrast media or Dextran through the guiding catheter. The images were digitally stored for offline analysis.

OCT image analysis. All OCT images were analyzed in the MGH OCT Core Laboratory by 2 experienced investigators (H.J. and F.A.) who were blinded to the angiographic data and clinical presentations. When there was discordance between the observers, a consensus reading was obtained from a third investigator.

Definition and classification. The plaque classification algorithm is shown in Figure 1. The current definitions of plaque erosion and calcified nodules have been well-established by pathology studies. To establish OCT criteria of OCT-erosion and OCT-CN, the resolution limits of OCT and the effects of prior treatment of patients with antithrombotics and thrombolysis had to be considered. A new set of OCT diagnostic criteria for OCT-erosion and OCT-CN was developed that incorporated the key aspects of the pathological definitions that could be visualized by OCT in the context of live treated patients. Because the OCT metrics for erosion are different from the pathological definition, we used the term "OCT-erosion" instead of erosion. The OCT-erosion was defined and categorized according to the absence of fibrous cap disruption and the presence of thrombus. Definite OCT-erosion was identified by the presence of attached thrombus overlying an intact and visualized plaque (Fig. 2). Probable OCT-erosion was defined by: 1) luminal surface irregularity at the culprit lesion in the absence of thrombus; or 2) attenuation of underlying plaque by thrombus without superficial lipid or calcification immediately proximal or distal to the site of thrombus (Fig. 3). This is in contrast to the pathological definition of erosion, which requires the presence of attached thrombus. Distinct from autopsy studies of acute coronary events, these subjects survived the acute event and were treated with antithrombotic therapy. As a result, the thrombus overlying the lesion might have been dissolved before OCT imaging. The OCT-CN was defined when fibrous cap disruption was detected over a calcified plaque characterized by protruding calcification, superficial calcium, and the presence of substantive calcium proximal and/or distal to the lesion (Fig. 4). Plaque rupture was identified by the presence of fibrous cap discontinuity with a clear cavity formed inside the plaque (Fig. 5).

The culprit lesions that did not meet the aforementioned criteria were classified as others, which included tight stenosis (Online Fig. 1) in the absence of any evidence of plaque rupture, OCT-erosion, or OCT-CN, spontaneous coronary artery dissection (Online Fig. 2), coronary spasm (Online Fig. 3), and fissure (Online Fig. 4).

Tissue characteristics of underlying plaque were defined with previously established criteria (7–9). Plaques were classified as: 1) fibrous (homogeneous, high backscattering

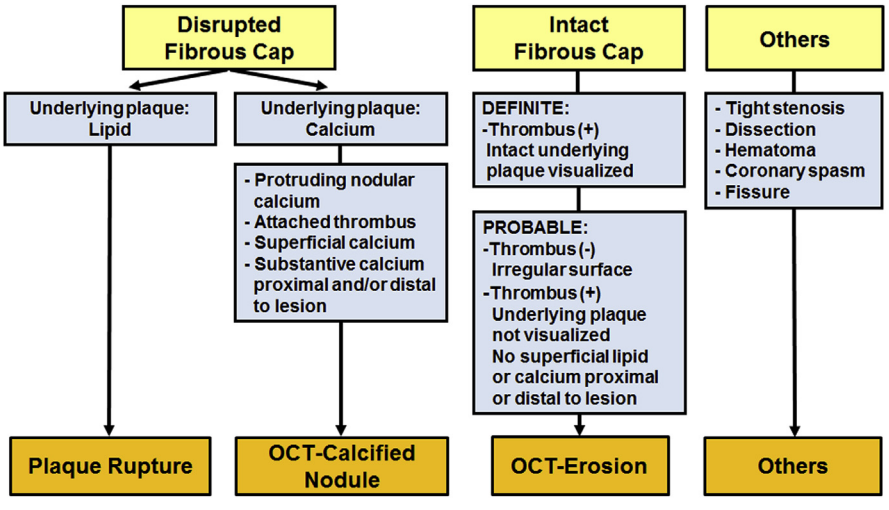

Figure 1 Plaque Classification Algorithm by OCT

OCT = optical coherence tomography.

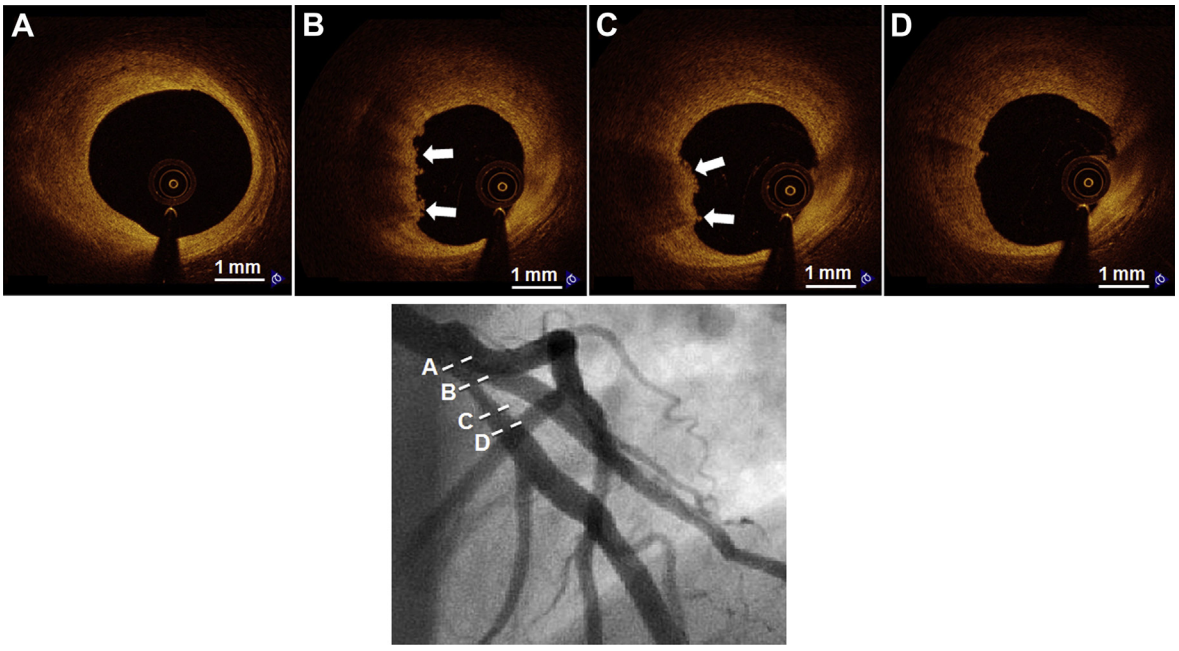

Figure 2 **Representative Case of "Definite OCT-Erosion"**

A 31-year-old man presented with non–ST-segment elevation myocardial infarction. Angiographic image **(bottom panel)** shows a moderate stenosis in the proximal left anterior descending coronary artery. Serial optical coherence tomography (OCT) cross-sectional images from proximal to distal of the culprit lesion indicate that no rupture is detected. Cross-sectional images indicate fibrous plaque (homogeneous high signal region) proximal **(A)** and distal **(D)** to thrombus. OCT-erosion is identified as an irregular lumen surface with attached mural thrombus **(arrows)** overlying a fibrous plaque **(B and C)**.

region); or 2) lipid (low-signal region with diffuse border). For each lipid plaque, the maximal lipid arc was measured. Lipid length was recorded on a longitudinal view. Thin-cap fibroatheroma was defined as a plaque with lipid content in ≥2 quadrants and the thinnest part of the fibrous cap measuring <65 μm. Intracoronary thrombus was defined as a mass (diameter >250 μm) attached to the luminal surface or floating within the lumen, including red (red blood cell-rich) thrombus, defined by high backscattering and high attenuation, or white (platelet-rich) thrombus, defined by homogeneous backscattering with low attenuation. Calcification was defined as an area with low backscattering signal and a sharp border inside a plaque. Microchannels were defined as signal-poor voids that were sharply delineated in multiple contiguous frames (9). Interobserver and intraobserver variability were assessed by the evaluation of all images by 2 independent observers and by the same observer at 2 separate time points, respectively. The inter-observer Kappa coefficients for thrombus, PR, definite OCT-erosion, probable OCT-erosion, and OCT-CN were 0.860, 0.885, 0.961, 0.877, and 0.927, respectively. The intra-observer Kappa coefficients for thrombus, PR, definite OCT-erosion, probable OCT-erosion, and OCT-CN were 0.953, 0.952, 0.970, 0.884, and 1.000, respectively.

Quantitative coronary angiography. Coronary angiograms were analyzed with the Cardiovascular Angiography Analysis System (Pie Medical Imaging B.V., Maastricht, the Netherlands). The reference diameter, minimum lumen diameter, diameter stenosis, area stenosis, and lesion length were measured.

Statistical analysis. All statistical analyses were performed by an independent statistician at the core laboratory. Categorical variables were presented as counts and proportions, and the comparisons were performed with a Fisher exact test. Continuous variables were presented as mean ± SD. The means of the continuous measurements were examined with the independent samples *t* test for 2-group comparisons, and analysis of variance for 3-group comparisons (plaque rupture, OCT-erosion, and OCT-calcified nodule) followed by post hoc test protected overall significance level of 0.05. A Bonferroni correction was used to control for multiple comparisons among the 3 groups (plaque rupture, OCT-erosion, and OCT-calcified nodule). All statistical analyses were performed with SPSS (version 17.0, SPSS, Inc., Chicago, Illinois). All p values were 2-sided.

Results

Baseline demographic data and laboratory results. The clinical characteristics of classified patients (PR, OCT-erosion, or OCT-CN) and patients with other atypical lesion characteristics are summarized in Table 1. There were no significant differences in all of the clinical characteristic variables between the 2 groups. The comparison of patient

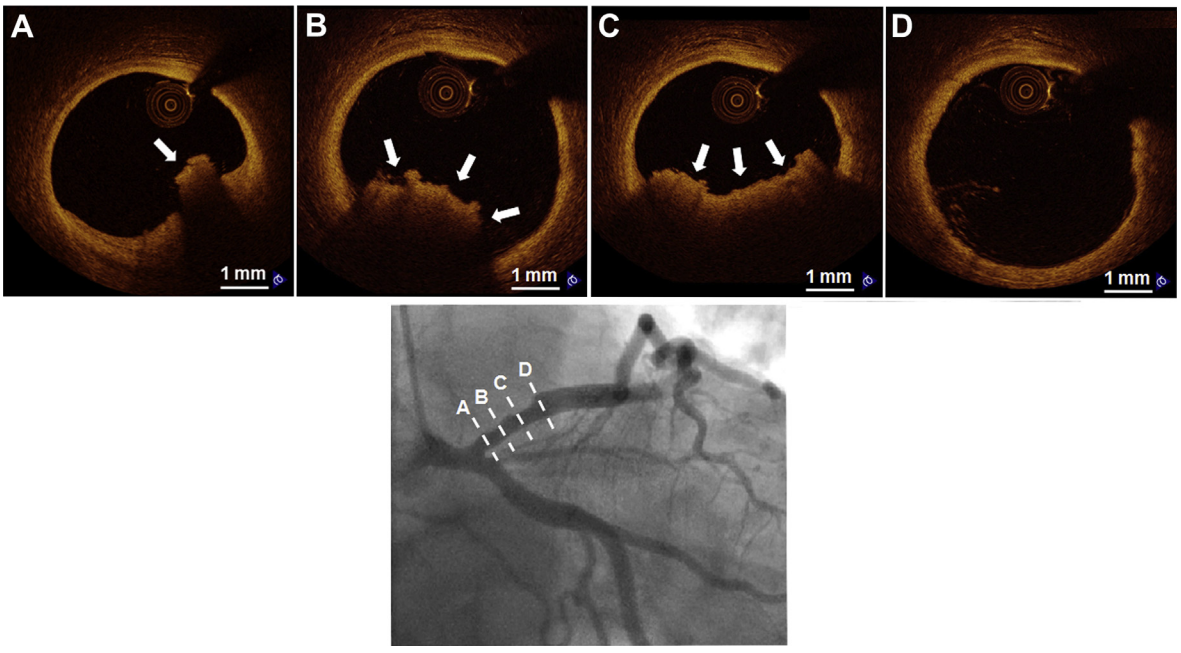

Figure 3 **Representative Case of "Probable OCT-Erosion"**

A 37-year-old male smoker presented with ST-segment elevation myocardial infarction. The angiographic image **(bottom panel)** shows a mild stenosis in the proximal left anterior descending coronary artery. Serial optical coherence tomography (OCT) cross-sectional images from proximal to distal of the culprit lesion show absence of detectable rupture **(A to D)**. Underlying plaque morphology is not well visualized, due to the presence of residual red thrombus **(A to C, arrows)**. The OCT images in the distal and proximal segments of the thrombotic lesions show the absence of superficial lipid and calcification **(A and D)**.

characteristics among PR, OCT-erosion, and OCT-CN are summarized in Table 2. Patients with OCT-erosion were the youngest compared with those with PR and OCT-CN. Patients with OCT-CN had the highest incidence of hypertension and chronic kidney disease compared with the other 2 groups. ST-segment elevation MI was more common in patients with PR than in those with OCT-erosion and OCT-CN. In contrast, the presentation of NSTE-ACS was predominant in patients with OCT-erosion and OCT-CN. Other variables, including sex, smoking, diabetes mellitus, hyperlipidemia, family history of coronary artery disease, prior MI, angiotensin-converting-enzyme inhibitor/angiotensin II receptor blocker use, and statin treatment, were comparable among the groups. Creatinine levels were highest in patients with OCT-CN, followed by those with PR and OCT-erosion. Other laboratory variables were comparable among the groups (Table 2).

Incidences of PR, OCT-erosion, and OCT-CN in patients with ACS. Among 126 culprit lesions studied, 55 (43.7%) lesions were classified as PR, 39 (31.0%) were classified as OCT-erosion, 10 (7.9%) were classified as OCT-CN, and 22 lesions (17.5%) were classified as others, which consisted of 8 (6.3%) lesions with tight stenosis, 3 (2.4%) with dissection, 2 (1.6%) with coronary spasm, 1 (0.8%) with fissure, 1 (0.8%) with Takotsubo, and the remaining 7 (5.6%) showing absence of any aforementioned characteristics. Among 39 OCT-erosion cases, definite OCT-erosion was detected in 23 (18.3%) patients, and probable OCT-erosion was detected in 16 (12.7%) patients (Fig. 6).

Angiographic findings. The lesion distribution and quantitative coronary angiography data are listed in Table 3. The OCT-erosion was more frequently detected in the left anterior descending artery, followed by the right coronary artery, and least in the left circumflex artery. Plaque rupture was equally distributed in the left anterior descending artery and right coronary artery. The reference diameter was comparable among the 3 groups. The minimum lumen diameter was largest in the OCT-erosion group, followed by the OCT-CN and PR groups ($p = 0.007$). The diameter stenosis was least severe in the OCT-erosion group, followed by the OCT-CN and PR groups ($p < 0.001$). No significant difference was seen in lesion length ($p = 0.424$).

Underlying plaque characteristics by OCT. The tissue characteristics of underlying plaque are shown in Table 4. In all rupture cases, the underlying plaques were lipid plaque. However, OCT-erosion was detected both in fibrous plaque and lipid plaque. Calcification was present in 22 of 55 (40.0%) PR, compared with 5 of 39 (12.8%) OCT-erosion ($p = 0.016$). Thin-cap fibroatheroma was observed in 67.3% of PR, 10.3% of OCT-erosion, and none of OCT-CN ($p < 0.001$). There was no significant difference in the presence of microchannels among the 3 groups. White thrombus was predominantly detected with OCT-erosion and OCT-CN, whereas red thrombus was found most

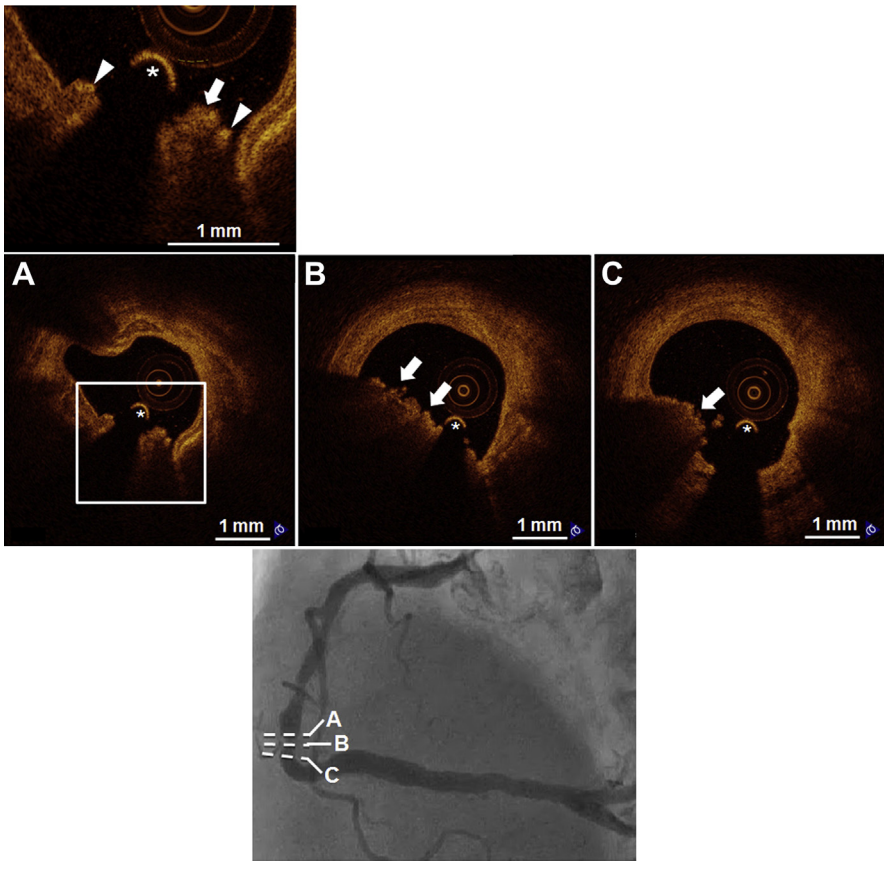

Figure 4 **Representative Case of "OCT-Calcified Nodule"**

A 75-year-old male smoker with unstable angina. Coronary angiogram angiography **(bottom panel)** demonstrated a complex lesion in the distal right coronary artery. Optical coherence tomography (OCT)-calcified nodule is identified as a nodular calcification **(A)** protruding into lumen through a disrupted fibrous cap **(arrowheads)** overlying superficial calcification with red thrombus **(B and C, arrows)** attached to the disrupted site. *Guidewire.

frequently with PR (Table 4). Quantitative OCT analysis of lipid plaque is shown in Table 5. Lipid plaque detected underneath OCT-erosion had a thicker fibrous cap ($p = 0.001$), smaller lipid arc ($p < 0.001$), and shorter lipid length ($p = 0.008$), as compared with those underneath the PR.

Discussion

To our knowledge, this study represents the first systematic effort to use OCT to characterize the morphologies of the 3 most common causes of ACS. The major findings of the present study are: 1) OCT provides unique insights in patients with plaque erosion and calcified nodule in addition to plaque rupture; 2) fibrous cap rupture was absent in more than one-half of culprit lesions (31% of lesions were classified as OCT-erosion, 8% were classified as OCT-CN, and the remaining 17% were classified as others and did not meet the criteria of PR, OCT-erosion, or OCT-CN); 3) patients with OCT-erosion were younger, had less severe stenosis, and less frequently presented with STEMI than those with PR; NSTE-ACS is the predominant presentation for the patients with OCT-erosion; and 4) lipid was less frequently detected in OCT-erosion than in PR. When lipid was present underneath OCT-erosion, overlying fibrous cap was thicker, lipid arc was smaller, and lipid length was shorter compared with those involved in PR.

In vivo detection of plaque erosion and calcified nodule with intravascular OCT. Coronary angiography is considered the gold standard diagnostic modality for the evaluation of patients presenting with ACS. However, angiography shows only the luminal outline and is not able to visualize intravascular structure. Although intravascular ultrasound is widely used to evaluate plaque morphology, including plaque burden and remodeling, the resolution is inadequate to characterize subtle changes in the vascular wall. For example, intravascular ultrasound cannot be used to detect mural thrombus, thin fibrous cap, and irregular or eroded surface. OCT is a promising modality for in vivo identification of these characteristics, which are predominantly located on the superficial surface of plaques. A limited number of imaging studies have evaluated the role of plaque erosion and calcified nodule in the pathophysiology of ACS

JACC Vol. 62, No. 19, 2013
November 5, 2013:1748–58

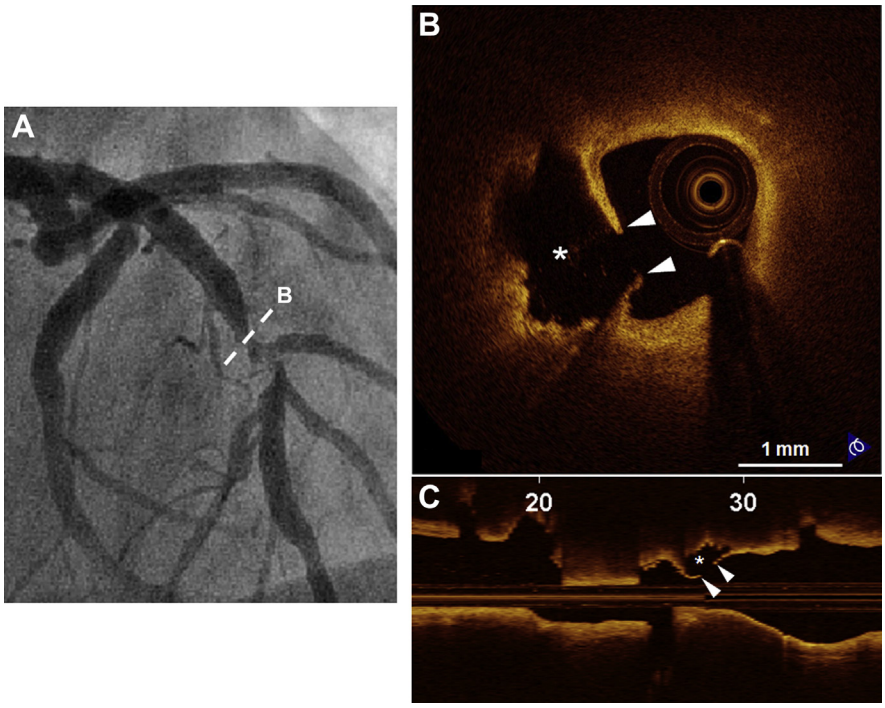

Figure 5 Representative Case of "Plaque Rupture"

A 57-year-old man presenting with ST-segment elevation myocardial infarction was treated with thrombolysis. **(A)** The coronary angiogram shows the culprit lesion in the mid left anterior descending coronary artery (**dashed line** indicates the ruptured site corresponding to **B**). Plaque rupture is identified on cross-sectional **(B)** and longitudinal **(C)** optical coherence tomography images by the disrupted fibrous-cap **(arrowheads)** and a cavity **(*)** formation inside the plaque.

in vivo (10,11). Moreover, the definitions used in those studies were based purely on pathological findings (loss of endothelial cell lines and/or dysfunction of endothelial cells) (1), which are beyond the resolution of OCT. In the present study, we established new diagnostic criteria for OCT-erosion and OCT-CN on the basis of pathological findings but also taking into account the limitations of OCT and the differences between live patient and postmortem evaluations. We used the proposed definitions to systematically classify the culprit lesions of patients with ACS. These definitions will be helpful for future OCT studies on investigating the underlying pathological mechanism of ACS.

Table 1 Patient Characteristics of the Classified Group and Others

	Classified (n = 104)	Others (n = 22)	p Value
Age, yrs	58.5 ± 12.2	60.0 ± 10.8	0.593
Male	84 (80.8%)	16 (72.7%)	0.395
Risk factors			
Smoking	54 (51.9%)	7 (46.7%)	0.103
Diabetes mellitus	24 (23.1%)	4 (18.2%)	0.781
Hyperlipidemia	67 (64.4%)	13 (59.1%)	0.635
Hypertension	60 (57.7%)	12 (54.5%)	0.816
Family history of CAD	12 (11.5%)	2 (9.1%)	1.000
Chronic kidney disease	5 (4.8%)	0 (0.0%)	0.586
Prior MI	16 (15.4%)	2 (9.1%)	0.737
Medications			
ACEI/ARB	31 (30.1%)	9 (40.9%)	0.323
Statin	33 (32.0%)	7 (31.8%)	1.000
Presentation			
STEMI	54 (51.9%)	7 (31.8%)	0.103
NSTE-ACS	50 (48.1%)	15 (68.2%)	

Values are mean ± SD or n (%). The p values were calculated with the use of *t* test for continuous variables and Fisher exact test for categorical variables.

ACE-I = angiotensin-converting-enzyme inhibitor; ARB = angiotensin II receptor blocker; CAD = coronary artery disease; MI = myocardial infarction; NSTE-ACS = non–ST-segment elevation acute coronary syndrome; STEMI = ST-segment elevation myocardial infarction.

Frequency of PR, OCT-erosion, and OCT-CN in patients with ACS. The most common underlying mechanisms responsible for acute coronary thrombosis are PR, plaque erosion, and calcified nodules (1). Plaque rupture is a widely recognized cause of ACS and is the most common morphology associated with acute coronary thrombosis. A previous autopsy study reported that the prevalence of PR and erosion in postmortem subjects with acute MI was 60% and 40%, respectively (5). Farb et al. (12) studied 50 consecutive SCD cases and found ruptures in 28 patients and erosions in 22. Another autopsy study conducted by Hisaki et al. (13) reported 70 PR and 54 erosions in 124 lesions of 122 postmortem patients with ACS. These pathological studies indicate that coronary thrombosis results from PR and plaque erosions in approximately 55% to 60% and 33% to 44% of cases, respectively. The incidence

Table 2 Baseline Characteristics of the Patients With PR, OCT-Erosion, and OCT-CN

	PR (n = 55)	OCT-Erosion (n = 39)	OCT-CN (n = 10)	p Value	p Value* PR vs. OCT-Erosion	p Value* OCT-Erosion vs. OCT-CN	p Value* PR vs. OCT-CN
Age, yrs	60.6 ± 11.5	53.8 ± 13.1	65.1 ± 5.0	0.005	0.019	0.023	0.802
Male	44 (80.0%)	32 (82.1%)	8 (80.0%)	0.968	N/A	N/A	N/A
Risk factors							
Smoking	26 (47.3%)	22 (56.4%)	6 (60.0%)	0.591	N/A	N/A	N/A
Diabetes mellitus	11 (20.0%)	9 (23.1%)	4 (40.0%)	0.385	N/A	N/A	N/A
Hyperlipidemia	41 (74.5%)	21 (53.8%)	5 (50.0%)	0.072	N/A	N/A	N/A
Hypertension	34 (61.8%)	17 (43.6%)	9 (90.0%)	0.020	0.285	0.036	0.435
Family history of CAD	7 (12.7%)	3 (7.7%)	2 (20.0%)	0.511	N/A	N/A	N/A
Chronic kidney disease	3 (5.5%)	0 (0.0%)	2 (20.0%)	0.029	0.792	0.115	0.498
Prior MI	7 (12.7%)	5 (12.8%)	4 (40.0%)	0.076	N/A	N/A	N/A
Medications							
ACEI/ARB	13 (23.6%)	12 (31.6%)	6 (60.0%)	0.068	N/A	N/A	N/A
Statin	19 (34.5%)	9 (23.7%)	5 (50.0%)	0.239	N/A	N/A	N/A
Presentation							
STEMI	39 (70.9%)	15 (38.5%)	0 (0.0%)	<0.001	0.008	0.063	<0.001
NSTE-ACS	16 (29.1%)	24 (61.5%)	10 (100%)				
Laboratory variables							
TC, mg/dl	178.9 ± 43.5	172.2 ± 55.2	157.6 ± 38.7	0.455	N/A	N/A	N/A
HDL-C, mg/dl	43.47 ± 17.2	50.92 ± 25.3	40.9 ± 5.2	0.165	N/A	N/A	N/A
LDL-C, mg/dl	102.5 ± 38.2	95.5 ± 36.7	93.7 ± 40.9	0.621	N/A	N/A	N/A
TG, mg/dl	180.9 ± 123.3	155.3 ± 88.7	164.1 ± 121.0	0.551	N/A	N/A	N/A
hs-CRP, mg/dl	0.91 ± 2.1	0.22 ± 0.16	0.55 ± 0.52	0.246	N/A	N/A	N/A
Creatinine, mg/dl	0.95 ± 0.17	0.90 ± 0.16	1.55 ± 1.74	0.004	1.000	0.003	0.006

Values are mean ± SD or n (%). Categorical variables were compared with the use of Fisher exact test. Continuous variables were compared with the use of analysis of variance (ANOVA) followed by post-hoc test only if the ANOVA $p < 0.05$. *The p values were adjusted by Bonferroni correction for multiple comparisons among the 3 groups (plaque rupture [PR], optical coherence tomography [OCT]-erosion, and OCT-calcified nodules [CN]).

HDL-C = high-density lipoprotein cholesterol; hs-CRP = high-sensitivity C-reactive protein; LDL-C = low-density lipoprotein cholesterol; TC = total cholesterol; TG = triglyceride; other abbreviations as in Table 1.

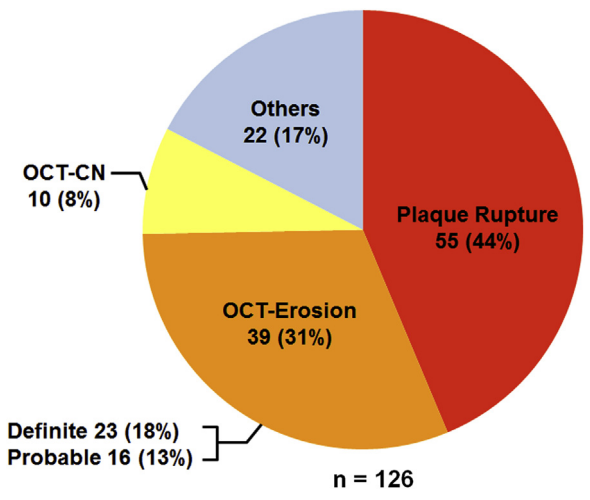

Figure 6 Incidence of Plaque Rupture, OCT-Erosion, and OCT-CN in Patients With ACS

Among the 126 culprit lesions, 55 (44%) lesions were classified as plaque rupture, 39 (31%) lesions were classified as optical coherence tomography (OCT)-erosion, 10 (8%) lesions were classified as OCT-calcified nodule (CN), and 22 (17%) lesions were classified as others. ACS = acute coronary syndrome.

of calcified nodules, which represent the least frequent cause of luminal thrombosis in ACS, was reported 4% to 7% (1). Our study showed that the prevalence of PR in patients with ACS was 44%, whereas those of OCT-erosion and OCT-CN were 31% and 8%, respectively. One of the reasons for the lower incidence of PR and OCT-erosion in the present study is likely the different population being studied. van der Wal et al. (5) studied only case subjects presenting with acute MI, whereas Farb et al. (12) studied case subjects dying of SCD, and Hisaki et al. (13) studied case subjects dying of ACS. We studied typical patients presenting with the full range of ACS. Another reason is the selection of patients on the basis of the ability to undergo OCT imaging. Patients with STEMI and large NSTEMI and sicker patients would be less likely to undergo pre-intervention OCT imaging. This biases the study toward a patient population with more stable presentation and more NSTE-ACS. The frequency of PR in our population might have been underestimated, given that PR is more common in STEMI.

Clinical characteristics of patients with PR, OCT-erosion, or OCT-CN. Autopsy studies have shown a significantly increased prevalence of plaque erosion in younger patients (<50 years old), especially in younger female

JACC Vol. 62, No. 19, 2013
November 5, 2013:1748–58

Table 3 Angiographic Findings

	PR (n = 55)	OCT-Erosion (n = 39)	OCT-CN (n = 10)	p Value	p Value* PR vs. OCT-Erosion	p Value* OCT-Erosion vs. OCT-CN	p Value* PR vs. OCT-CN
Lesion location							
LAD	27 (49.1%)	28 (71.8%)	6 (60.0%)	0.012	0.006	1.000	1.000
RCA	20 (36.4%)	6 (15.4%)	3 (30%)				
LCX	8 (14.5%)	5 (12.8%)	1 (10.0%)				
QCA data							
RVD, mm	3.6 ± 0.9	3.7 ± 1.0	3.2 ± 0.7	0.242	N/A	N/A	N/A
MLD, mm	1.0 ± 0.5	1.4 ± 0.6	1.2 ± 0.6	0.007	0.005	0.824	1.000
Diameter stenosis, %	68.8 ± 12.9	55.4 ± 14.7	66.1 ± 13.5	<0.001	<0.001	0.096	1.000
Lesion length, mm	16.4 ± 5.8	15.0 ± 5.0	17.1 ± 5.5	0.424	N/A	N/A	N/A

Values are n (%) or mean ± SD. Categorical variables were compared with the use of Fisher exact test. Continuous variables were compared with the use of ANOVA followed by post hoc test only if the ANOVA $p < 0.05$. *p values were adjusted by Bonferroni correction for multiple comparisons among the 3 groups (PR, OCT-erosion, and OCT-CN) only if p value for the overall 3-group test <0.05.

LAD = left anterior descending coronary artery; LCX = left circumflex artery; MLD = minimum lumen diameter; RCA = right coronary artery; QCA = quantitative coronary angiogram analysis; RVD = reference vessel diameter; other abbreviations as in Tables 1 and 2.

patients (12). Burke et al. (14) reported that smoking was associated with plaque erosion among female victims of sudden death. In the present study, we also found that patients with OCT-erosion are younger (<55 years of age) than those with rupture. However, OCT-erosions were not found more frequently in women than in men. This discrepancy could be due to the difference in populations studied (cases of SCD vs. patients with ACS). Specifically, subjects evaluated in the postmortem studies were significantly younger than typical patients with a history of CAD and/or ACS. Furthermore, SCD is dependent on not only the plaque pathology but also the relative thrombotic state of the patient and their propensity to develop a fatal arrhythmia. This raises the possibility of selection bias in evaluating the clinical characteristics of these patients. The population in this study was more representative of patients who are seen in clinical practice. Alternatively, we might be classifying lesions as plaque erosions by OCT that would not be diagnosed as such by pathology. However, we found that the frequency of STEMI was significantly higher in the patients with PR than others. In contrast, NSTE-ACS was predominant in patients with OCT-erosion and OCT-CN. These differences were consistent with the previous study, which reported that patients with plaque erosion had less STEMI on admission and less Q-wave MI than those with ruptures (15). Pathologically, calcified nodules are heavily calcified lesions consisting of calcified plates and overlying disrupted thin fibrous cap and thrombus and are more common in older individuals (1,16). Recent studies showed that coronary calcification was more frequent and severe in patients with chronic kidney disease compared with those with normal renal function (17,18). These results support our findings that OCT-CN was observed more frequently in older patients (>65 years of age) with hypertension, chronic renal disease, and higher level of creatinine.

Underlying plaque characteristics of ACS. Previous work showed that plaque erosion occurred over lesions rich in smooth muscle cells and proteoglycans. The deep intima of the eroded plaque often showed extracellular lipid pools, but necrotic cores were uncommon (1). In the present study, all PR were detected in the context of lipid plaques. In contrast, 44% of OCT-erosions were detected in lipid plaques, and 56% were detected in fibrous plaques. This finding is consistent with pathological results that necrotic core was detected in 100% of PR and 47% of plaque erosion (6). Autopsy studies have shown that more than 88% of coronary thrombi overlying plaque erosions exhibited late stages of healing characterized by invasion of organized layers of smooth muscle cells, endothelial cells with varying degrees of platelet/fibrin layering. In patients with PR, only 50% of

Table 4 OCT Findings of Underlying Plaque Characteristics

	PR (n = 55)	OCT-Erosion (n = 39)	OCT-CN (n = 10)	p Value	p Value* PR vs. OCT-Erosion	p Value* OCT-Erosion vs. OCT-CN	p Value* PR vs. OCT-CN
Fibrous plaque	0 (0.0%)	22 (56.4%)	10 (100%)	<0.001	<0.001	0.027	<0.001
Lipid plaque	55 (100%)	17 (43.6%)	0 (0.0%)	<0.001	<0.001	0.027	<0.001
TCFA	37 (67.3%)	3 (10.3%)	0 (0.0%)	<0.001	<0.001	1.000	<0.001
Calcification	22 (40.0%)	5 (12.8%)	10 (100%)	<0.001	0.016	<0.001	0.001
Microchannel	21 (38.2%)	7 (17.9%)	2 (6.7%)	0.083	N/A	N/A	N/A
Thrombus	45 (81.8%)	33 (84.6%)	10 (100%)	0.242	N/A	N/A	N/A
Red thrombus	39 (70.9%)	6 (15.4%)	4 (40.0%)	<0.001	<0.001	0.541	0.226
White thrombus	6 (10.9%)	27 (69.2%)	6 (60.0%)	<0.001	<0.001	1.000	0.005

Values are n (%). *The p values were calculated by Fisher exact test and adjusted by Bonferroni correction for multiple comparisons within 3 groups (PR, OCT-erosion, and OCT-CN) only if p value for the overall 3-group test <0.05.

TCFA = thin-cap fibroatheroma; other abbreviations as in Table 2.

Table 5 OCT Measurements of Lipid Plaque

	PR (n = 55)	OCT-Erosion (n = 17)	p Value
Fibrous cap thickness, μm	60.4 ± 16.6	169.3 ± 99.1	0.001
Maximal lipid arc, °	275.8 ± 60.4	202.8 ± 73.6	<0.001
Lipid length, mm	13.1 ± 4.5	9.7 ± 23.2	0.008

Values are mean ± SD.

thrombi showed evidence of healing (6). In our study, fibrin rich red thrombus was frequently found over ruptured plaque, whereas platelet rich white thrombus was the predominant type of thrombus formed over OCT-erosion and OCT-CN.

Clinical implication. The distinct pathological features and clinical characteristics associated with PR, OCT-erosion, and OCT-CN suggest that they might be caused by different pathophysiologic processes and therefore might merit tailored treatment. The present study also showed that the presentation with STEMI was more common in patients with PR, whereas NSTE-ACS was more frequent in those with OCT-erosion and OCT-CN. Plaque rupture induces massive thrombus formation at the culprit site. In contrast, OCT-erosion seems to result in less thrombus burden, preserved vascular structure, and larger lumen (6,12). Given these features, it is conceivable that patients with OCT-erosion might be stabilized by effective antithrombotic treatment without stent implantation, thereby avoiding both early and late complications associated with stent. However, further evidence is needed to support our findings to guide clinical practice.

Study limitations. First, the present study involves a small cohort with ACS and is highly selected on the basis of the ability to undergo OCT imaging. However, this is the first in vivo study to systematically investigate and classify the underlying plaque characteristics of ACS lesions with intravascular imaging. Second, the definitions of plaque erosion and calcified nodule as detected by OCT were not validated by pathology in these patients. True pathological validation is impossible, because of the fundamental difference in analyzing patients who died from ACS and those who survived and have been treated with antithrombotics. Specifically, intracoronary thrombus burden in patients treated for ACS would have been altered by treatment. Therefore, the diagnostic criteria used were established in collaboration with pathologist (R.V.), imaging specialist (J.N.), and clinicians. Third, the presence of thrombus overlying the culprit lesion might reduce the ability to assess the underlying plaque characteristics by OCT. Therefore, patients with massive occlusive thrombosis were excluded from our study. In addition, the pathological definition of calcified nodules requires a fracture of the underlying calcified plate. OCT is not an ideal tool to visualize a deep fractured calcified plate. Finally, the absence of endothelial cells is a key pathological criterion for erosion. Despite its high resolution, current OCT technique cannot detect individual endothelial cells. As a result, the OCT definition of plaque erosion was based primarily on a diagnosis of exclusion requiring the absence of a fibrous cap rupture.

Conclusions

This study demonstrates that OCT is a promising modality for in vivo diagnosis of PR, OCT-erosion, and OCT-CN. OCT-erosion is a frequent finding in patients with ACS, which accounts for 31% of cases in the present study. OCT-erosion is more frequent in younger patients with NSTE-ACS and has less severe luminal stenosis, compared with PR. In addition, OCT-erosion has higher incidence of platelet-rich thrombus. OCT-CN is the least common etiology for ACS and is more common in older patients.

Acknowledgment

The authors thank Christina M. Kratlian for her editorial expertise on the manuscript.

Reprint requests and correspondence: Dr. Bo Yu, Department of Cardiology, The 2nd Affiliated Hospital of Harbin Medical University, Key Laboratory of Myocardial Ischemia (Harbin Medical University), Chinese Ministry of Education, Harbin, People's Republic of China, 150086. E-mail: yubodr@163.com OR Dr. Ik-Kyung Jang, Massachusetts General Hospital, Cardiology Division, 55 Fruit Street GRB 800, Boston, Massachusetts 02114. E-mail: ijang@partners.org.

REFERENCES

1. Virmani R, Kolodgie FD, Burke AP, Farb A, Schwartz SM. Lessons from sudden coronary death: a comprehensive morphological classification scheme for atherosclerotic lesions. Arterioscler Thromb Vasc Biol 2000;20:1262–75.
2. Naghavi M, Libby P, Falk E, et al. From vulnerable plaque to vulnerable patient: a call for new definitions and risk assessment strategies: Part I. Circulation 2003;108:1664–72.
3. Virmani R, Burke AP, Farb A, Kolodgie FD. Pathology of the vulnerable plaque. J Am Coll Cardiol 2006;47:C13–8.
4. Davies MJ. Anatomic features in victims of sudden coronary death. Coronary artery pathology. Circulation 1992;85:I19–24.
5. van der Wal AC, Becker AE, van der Loos CM, Das PK. Site of intimal rupture or erosion of thrombosed coronary atherosclerotic plaques is characterized by an inflammatory process irrespective of the dominant plaque morphology. Circulation 1994;89:36–44.
6. Kramer MC, Rittersma SZ, de Winter RJ, et al. Relationship of thrombus healing to underlying plaque morphology in sudden coronary death. J Am Coll Cardiol 2010;55:122–32.
7. Jang IK, Bouma BE, Kang DH, et al. Visualization of coronary atherosclerotic plaques in patients using optical coherence tomography: comparison with intravascular ultrasound. J Am Coll Cardiol 2002;39:604–9.
8. Yabushita H, Bouma BE, Houser SL, et al. Characterization of human atherosclerosis by optical coherence tomography. Circulation 2002;106:1640–5.
9. Tearney GJ, Regar E, Akasaka T, et al. Consensus standards for acquisition, measurement, and reporting of intravascular optical coherence tomography studies: a report from the International Working Group for Intravascular Optical Coherence Tomography Standardization and Validation. J Am Coll Cardiol 2012;59:1058–72.

10. Kubo T, Imanishi T, Takarada S, et al. Assessment of culprit lesion morphology in acute myocardial infarction: ability of optical coherence tomography compared with intravascular ultrasound and coronary angioscopy. J Am Coll Cardiol 2007;50:933–9.
11. Rathore S, Terashima M, Matsuo H, et al. Association of coronary plaque composition and arterial remodelling: a optical coherence tomography study. Atherosclerosis 2012;221:405–15.
12. Farb A, Burke AP, Tang AL, et al. Coronary plaque erosion without rupture into a lipid core: a frequent cause of coronary thrombosis in sudden coronary death. Circulation 1996;93:1354–63.
13. Hisaki R, Yutani C. Plaque morphology of acute coronary syndrome. J Atheroscler Thromb 1998;4:156–61.
14. Burke AP, Farb A, Malcom GT, Liang Y, Smialek J, Virmani R. Effect of risk factors on the mechanism of acute thrombosis and sudden coronary death in women. Circulation 1998;97:2110–6.
15. Hayashi T, Kiyoshima T, Matsuura M, et al. Plaque erosion in the culprit lesion is prone to develop a smaller myocardial infarction size compared with plaque rupture. Am Heart J 2005;149:284–90.
16. Xu Y, Mintz GS, Tam A, et al. Prevalence, distribution, Predictors, and outcomes of patients with calcified nodules in native coronary arteries: a 3-vessel intravascular ultrasound analysis from Providing Regional Observations to Study Predictors of Events in the Coronary Tree (PROSPECT). Circulation 2012;126:537–45.
17. Budoff MJ, Rader DJ, Reilly MP, et al. Relationship of estimated GFR and coronary artery calcification in the CRIC (Chronic Renal Insufficiency Cohort) study. Am J Kidney Dis 2011;58:519–26.
18. Koukoulaki M, Papachristou E, Kalogeropoulou C, et al. Increased prevalence and severity of coronary artery calcification in patients with chronic kidney disease stage III and IV. Nephron Extra 2012;2:192–204.

Key Words: acute coronary syndrome ■ calcified nodule ■ optical coherence tomography ■ plaque erosion ■ plaque rupture.

APPENDIX

For a list of the Massachusetts General Hospital OCT Registry and supplemental figures, please see the online version of this article.